
Density Uncertainty Layers for Reliable Uncertainty Estimation

Yookoon Park

Department of Computer Science
Columbia University
New York, NY 10027, USA
yookoon.park@columbia.edu

David M. Blei

Department of Computer Science, Statistics
Columbia University
New York, NY 10027, USA
david.blei@columbia.edu

Abstract

Assessing the predictive uncertainty of deep neural networks is crucial for safety-related applications of deep learning. Although Bayesian deep learning offers a principled framework for estimating model uncertainty, the approaches that are commonly used to approximate the posterior often fail to deliver reliable estimates of predictive uncertainty. In this paper we propose a novel criterion for predictive uncertainty, that a model’s predictive variance should be grounded in the empirical density of the input. It should produce higher uncertainty for inputs that are improbable in the training data and lower uncertainty for those inputs that are more probable. To operationalize this criterion, we develop the density uncertainty layer, an architectural element for a stochastic neural network that guarantees that the density uncertain criterion is satisfied. We study neural networks with density uncertainty layers on the CIFAR-10 and CIFAR-100 uncertainty benchmarks. Compared to existing approaches, we find that density uncertainty layers provide reliable uncertainty estimates and robust out-of-distribution detection performance.

1 Introduction

The success of deep learning in a range of applications has spurred significant interest in deploying neural network models in real-world prediction scenarios. But in high-stakes domains, such as health-care, finance, and autonomous systems, both the model’s prediction and its predictive uncertainty are crucial. An important challenge is that conventional neural networks lack a robust mechanism for quantifying their uncertainty, and they tend to produce overconfident predictions [Guo et al., 2017, Ovadia et al., 2019]. This paper is about how to produce good estimates of predictive uncertainty.

Why is this a problem? Bayesian deep learning offers a principled framework for quantifying the uncertainty of deep neural networks by incorporating uncertainty about the model parameters [Graves, 2011, Welling and Teh, 2011, Neal, 2012, Blundell et al., 2015]. However, the variational inference methods commonly employed for approximating the posterior [Graves, 2011, Blundell et al., 2015] often fall short of providing reliable predictive uncertainty [Foong et al., 2019b, Ober and Rasmussen, 2019]. To see this on a toy problem, see Figure 1a.

In this work, we propose a novel criterion for reliable uncertainty estimation and a new architectural element for stochastic neural networks to satisfy it. The *density uncertainty criterion* posits that a model’s predictive uncertainty should be grounded in the empirical density of the input. We should see higher uncertainty for improbable inputs and lower for more probable ones. As motivation, we will illustrate how Bayesian linear regression inherently adheres to the criterion.

We then develop the *density uncertainty layer*, an architectural element for stochastic neural networks that is designed to satisfy the density uncertainty criterion. The idea is to fit an energy-based model

of input and then satisfy the density uncertainty criterion via a constraint on the predictive variance produced by the approximate posterior. Density uncertainty layers satisfy the uncertainty criterion and serve as a flexible building block for uncertainty-aware deep neural networks. On the same toy problem, see Figure 1d.

We study deep neural networks with density uncertainty layers on the CIFAR-10 and CIFAR-100 uncertainty benchmarks. When compared to existing methods for estimating predictive uncertainty in neural networks [Blundell et al., 2015, Kingma et al., 2015, Gal and Ghahramani, 2016, Dusenberry et al., 2020], we find that the uncertainty-aware neural networks proposed here provide better estimates of uncertainty and robust out-of-distribution (OOD) detection.

Contributions. In summary, this paper makes the following contributions.

1. We propose a novel uncertainty criterion for reliable uncertainty estimation, asserting that a model’s predictive uncertainty should be grounded in the empirical density of the input.
2. We present the density uncertainty layer, a stochastic neural network layer that uses density estimate of the input to satisfy the density uncertainty criterion.
3. We study density uncertainty layers on the CIFAR-10 and CIFAR-100 uncertainty benchmarks. On both benchmarks, this method performs better than existing approaches.

2 Density Uncertainty Layers for Uncertainty Estimation

2.1 Motivation: Bayesian Linear Regression Performs Density Estimation

In this section, we illustrate how Bayesian uncertainty is grounded in the observed density of the input. This observation will motivate us to subsequently formalize the concept as a novel criterion for reliable uncertainty estimation.

Consider a Bayesian linear regression model with the input $\mathbf{X} \in \mathbb{R}^{N \times D}$, the target $\mathbf{y} \in \mathbb{R}^N$, and the weight $w \in \mathbb{R}^D$:

$$p(w) = \mathcal{N}(w|0, \alpha^{-1}I), \quad (1)$$

$$p(\mathbf{y}|\mathbf{X}, w) = \prod_{i=1}^N \mathcal{N}(y_i|w^T x_i, \beta^{-1}), \quad (2)$$

The posterior distribution of the weight w given the observations $\mathcal{D} = \{\mathbf{X}, \mathbf{y}\}$ is [Bishop, 2006]

$$p(w|\mathcal{D}) = \mathcal{N}(w|\mu, \Lambda^{-1}), \quad (3)$$

$$\mu = \beta \Lambda^{-1} \mathbf{X}^T \mathbf{y}, \quad (4)$$

$$\Lambda = \beta \mathbf{X}^T \mathbf{X} + \alpha I. \quad (5)$$

The posterior predictive distribution for a test input x_* is obtained by marginalizing out the weight from the posterior joint:

$$p(y_*|x_*, \mathcal{D}) = \int p(y_*, w|x_*, \mathcal{D}) dw \quad (6)$$

$$= \mathcal{N}(y_*|\mu^T x_*, \beta^{-1} + x_*^T \Lambda^{-1} x_*) \quad (7)$$

At this point, we establish the connection between the Bayesian predictive uncertainty and the empirical input density by rewriting the predictive variance in Equation (7) as:

$$\text{Var}[y_*|x_*, \mathcal{D}] = \beta^{-1} + x_*^T (\beta \mathbf{X}^T \mathbf{X} + \alpha I)^{-1} x_* \quad (8)$$

$$= \frac{1}{\beta} + \frac{2}{\beta N} E(x_*), \quad (9)$$

$$\text{for } E(x_*) = \frac{1}{2} x_*^T \hat{\Sigma}^{-1} x_*, \text{ and } \hat{\Sigma} = \frac{1}{N} (\mathbf{X}^T \mathbf{X} + \frac{\alpha}{\beta} I). \quad (10)$$

Here $E(x)$ is an energy function, an unnormalized negative log density of x such that:

$$p_{\text{gen}}(x) \propto \exp(-E(x)) = \exp(-\frac{1}{2} x^T \Sigma^{-1} x). \quad (11)$$

This energy model assumes the data come from a zero-mean normal distribution $x \sim \mathcal{N}(0, \Sigma)$ with covariance Σ . Notably, $\hat{\Sigma} = (\mathbf{X}^T \mathbf{X} + (\alpha/\beta)I)/N$ as in Equation (10) is the MAP estimate of the input covariance given the observations \mathbf{X} . This reveals that the Bayesian linear model derives its predictive uncertainty from the Gaussian input density estimate. Consequently, the uncertainty will be high for test inputs that are improbable in the empirical density and low for those that are more probable, providing intuitive and reliable predictive uncertainty. In the following sections, we build upon this principle to develop a novel criterion for reliable uncertainty estimation.

2.2 The Density Uncertainty Criterion

While Bayesian uncertainty for a linear model has desirable properties, when variational inference (VI) is applied for approximating the intractable parameter posterior $p(\theta|\mathcal{D})$ in deep neural networks, it often fails to provide reliable uncertainty estimates [Foong et al., 2019a, Ober and Rasmussen, 2019]. This issue is also evident in a toy regression problem (Figure 1) where the VI baselines fail to accurately capture the density of the data in their predictive uncertainty.

Towards reliable uncertainty estimation for deep neural networks, we propose a novel uncertainty criterion asserting that a model’s predictive uncertainty should be grounded in the observed density of the input. To formalize the concept, we first introduce an auxiliary energy-based model of the input:

$$p_{\text{gen}}(x; \omega) \propto \exp(-E(x; \omega)), \quad (12)$$

where the generative parameter ω is fitted to the training data x_1, \dots, x_N . We will henceforth omit the generative parameter ω for simplicity.

We now establish the *density uncertainty criterion* for a parameterized model $f(x; \theta)$ with a distribution on the parameters $q(\theta)$ as

$$\text{Var}_{q(\theta)}[f(x; \theta)] \propto E(x) \text{ for all } x \in \mathcal{X}. \quad (13)$$

This criterion posits that the predictive uncertainty should be proportional to the energy of the input, for a non-negative energy function $E(x) \geq 0$. This results in high predictive uncertainty for inputs that are improbable in the empirical distribution and low uncertainty for those inputs that are more probable. As illustrated in Section 2.1, Bayesian linear model is a notable example that inherently satisfies the density uncertainty criterion of Equation (13).

By integrating the density uncertainty criterion into the evidence lower-bound (ELBO), we obtain the constrained optimization objective:

$$\begin{aligned} \arg \max_{q \in \mathcal{Q}} \mathbb{E}_{q(\theta)} \left[\sum_{i=1}^N \log p(y_i | f(x_i; \theta)) \right] + D_{KL}(q(\theta) \| p(\theta)) \\ \text{subject to } \text{Var}_{q(\theta)}[f(x; \theta)] \propto E(x) \text{ for all } x \in \mathcal{X}, \end{aligned} \quad (14)$$

The constraint in Equation (14) directly enforces the predictive distributions to adhere to the density uncertainty criterion, in contrast to VI which only focuses on the parameter uncertainty. This approach ensures that the predictive uncertainty is consistently derived from the empirical density of the input, yielding reliable uncertainty estimates.

Example: Bayesian linear regression Revisiting the Bayesian linear regression example (Section 2.1), the parameter distribution $q(w)$ that satisfies the density uncertainty criterion is

$$q(w) = \mathcal{N}(\mu, \gamma \Sigma^{-1}), \text{ where } \Sigma = \frac{1}{N}(\mathbf{X}^T \mathbf{X} + \frac{\alpha}{\beta} I), \quad (15)$$

where γ is a scaling scalar and μ is a trainable parameter. The posterior precision of the weight is now tied to the empirical covariance estimate of the input. This results in the predictive variance of

$$\text{Var}_{q(w)}[f(x_*; w)] \propto E(x_*) = \frac{1}{2} x_*^T \Sigma^{-1} x_*, \quad (16)$$

where the Gaussian energy model E is fitted to the training data. Thus, the constraint on the precision matrix acts as a form of posterior regularization that encodes our density uncertainty criterion. It is worth noting that the constrained parameter posterior (Equation (15)) recovers the true posterior in Bayesian linear regression (Equation (3)).

Reparametrized objective More generally, we introduce the reparametrized version of the objective for a stochastic function $f(x, \epsilon; \phi)$ with a deterministic parameter ϕ and noise input ϵ :

$$\begin{aligned} \arg \max_{\phi} \mathbb{E}_{q(\epsilon)} \left[\sum_{i=1}^N \log p(y_i | f(x_i, \epsilon; \phi)) \right] + D_{KL}(q(\epsilon) \| p(\epsilon)) \\ \text{subject to } \text{Var}_{q(\epsilon)}[f(x, \epsilon; \phi)] \propto E(x) \text{ for all } x \in \mathcal{X}, \end{aligned} \quad (17)$$

A broad class of $q(\theta)$ such as normal distributions admits this reparametrization. In this setting, the exogenous noise ϵ sources the stochasticity of the model and exposes the deterministic model parameter ϕ . The reparametrized objective offers more flexibility in how we incorporate noise into the model while adhering to the density uncertainty criterion. For example, we may choose to directly inject noise into the low-dimensional function output instead of sampling the high-dimensional parameters, thereby improving the computational efficiency and reducing the gradient variance [Kingma et al., 2015]. Therefore, we default to this form in the remainder of the paper.

2.3 The Density Uncertainty Layer

It is now left to select an appropriate energy model $E(x)$ and the structure of a stochastic function $f(x, \epsilon; \phi)$ for deep neural networks. We view a neural network as a composition of linear layers and nonlinear activation functions: $\Omega = f_{L+1} \circ \pi \circ f_L \circ \pi \circ \dots \circ \pi \circ f_1$ where f_ℓ is a stochastic linear layer at layer ℓ and π is the nonlinear activation function such as ReLU. Instead of enforcing the uncertainty criterion (Equation (13)) on the neural network Ω , we propose to make the individual linear layers f_1, f_2, \dots, f_{L+1} stochastic and adhere to the density uncertainty criterion layer-wise.

Motivated by the insights in Section 2.1 that Bayesian linear regression involves a Gaussian energy model of the input, we pair each linear layer f_ℓ with a Gaussian energy model E_ℓ and impose the uncertainty criterion layer-wise:

$$\begin{aligned} \arg \max_{\phi} \mathbb{E}_{q(\epsilon)} \left[\sum_{i=1}^N \log p(y_i | \Omega(x_i, \epsilon; \phi)) \right] + D_{KL}(q(\epsilon) \| p(\epsilon)) \\ \text{subject to } \text{Var}_{q(\epsilon_\ell)}[f_\ell(h_{\ell-1}, \epsilon_\ell; \phi_\ell)] \propto E_\ell(h_{\ell-1}) \text{ for all } h_{\ell-1} \in \mathcal{H} \text{ and } \ell = 1, \dots, L+1, \end{aligned} \quad (18)$$

where ϕ encompasses the deterministic weights of the neural network and the posterior parameters of the noise distributions, while ϵ involves all noise variables in the network. This design is based on several key observations: First, a Gaussian energy model provides a smooth uncertainty landscape while being sufficiently expressive to capture correlations among input dimensions. Second, the Gaussian energy facilitates efficient training and energy evaluation. Third, injecting noise into the individual layers fosters functional diversity and stochastic regularization effect. Lastly, the complexity of the uncertainty landscape grows naturally with the model complexity as the number of layers in the neural network increases.

We are now prepared to introduce the *density uncertainty layer*, a stochastic neural network architecture that by design satisfies the density uncertainty criterion in Equation (18):

$$\begin{aligned} f_\ell^j(h_{\ell-1}, \epsilon_\ell^j; w_\ell^j) &= w_\ell^j \cdot h_{\ell-1} + \epsilon_\ell^j \sqrt{E(h_{\ell-1})} + \eta_\ell^j, \text{ for } j = 1, \dots, M_\ell \\ \text{where } E_\ell(h_{\ell-1}) &= \frac{1}{2} h_{\ell-1}^T \Sigma_{\ell-1}^{-1} h_{\ell-1} \text{ and } q(\epsilon_\ell^j) = \mathcal{N}(0, \gamma_\ell^j), q(\eta_\ell^j) = \mathcal{N}(0, \beta_\ell^j). \end{aligned} \quad (19)$$

w_ℓ^j is the weight vector for the j -th hidden unit at layer ℓ and M_ℓ is the number of hidden units in the layer. $E_\ell(h_{\ell-1})$ is the Gaussian energy model with the parameter $\Sigma_{\ell-1}$ estimating the covariance of the layer's input $h_{\ell-1}$. We introduce two noise components: ϵ_ℓ^j that scales with the energy and η_ℓ^j that is independent of the energy. This results in the predictive variance of the layer

$$\text{Var}_{q(\epsilon_\ell)}[f_\ell(h_{\ell-1}, \epsilon_\ell; \phi_\ell)] = \gamma_\ell^j E_\ell(h_{\ell-1}) + \beta_\ell^j, \quad (20)$$

which satisfies the density uncertainty criterion as the bias term β_ℓ^j can be absorbed into the energy function. The posterior noise variance parameters $\gamma_\ell^j, \beta_\ell^j$ are optimized using the ELBO, granting the model the flexibility to adjust the noise variance for individual hidden units in the layer. While we assume Gaussian noise for simplicity, we may potentially incorporate other noise distributions such as heavy-tailed ones [Dusenberry et al., 2020] for better robustness.

2.4 Implementing the Density Uncertainty Layer

We adopt the LDL parametrization for the precision matrix $\Sigma_\ell^{-1} = L_\ell D_\ell L_\ell^T$ in the layer-wise Gaussian energy models, where L_ℓ is a lower-triangular matrix with 1 in the diagonal, and D_ℓ is a diagonal matrix with non-negative elements. This parametrization admits efficient energy evaluation

$$E_\ell(h_{\ell-1}) = \frac{1}{2} \|D_{\ell-1}^{\frac{1}{2}} L_{\ell-1}^T h_{\ell-1}\|_2^2, \quad (21)$$

without needing to invert the covariance matrix and simplifies the calculation of the log determinant of the covariance matrix as $\log |\Sigma_\ell| = -\sum_j \log D_\ell^{jj}$. For a convolutional architecture, we replace the matrix-vector product $L_{\ell-1}^T h_{\ell-1}$ with a linear masked convolution [Van den Oord et al., 2016] to adapt the energy model. This is motivated by the observation that the lower-triangular elements of L_ℓ can be interpreted as a linear autoregressive model of the input [Pourahmadi, 1999]. Then the energy can be computed as a squared sum of the residuals of the autoregressive model, weighted by $D_{\ell-1}^{-1}$. The main computational overhead of density uncertainty layers comes from the matrix-vector product in Equation (21), which is roughly equivalent to that of a deterministic neural network layer.

Optimization The structure of the density uncertainty layer (Equation (19)) inherently satisfies the density uncertainty constraint, simplifying the constrained optimization objective (Equation (18)) to

$$\mathcal{L}_{\text{ELBO}}(\phi) = \mathbb{E}_{q(\epsilon)} \left[\sum_{i=1}^N \log p(y_i | \Omega(x_i, \epsilon; \phi)) \right] + D_{KL}(q(\epsilon) \| p(\epsilon)) \quad (22)$$

We assume Gaussian priors with a shared variance for the noise variables. Concurrently, the generative parameters ω of the layer-wise energy models are optimized using the generative objective:

$$\mathcal{L}_{\text{gen}}(\omega) = \sum_{i=1}^N \sum_{\ell=1}^{L+1} \mathbb{E}_{q(\epsilon)} [\log p_{\text{gen}}(h_\ell; \omega_\ell)] + \log p(\omega_\ell), \quad (23)$$

where $p_{\text{gen}}(h_\ell; \omega_\ell) = \exp(-E(h_\ell))$ is the Gaussian energy distribution for the input at layer ℓ and $p(\omega_\ell)$ is a prior on the generative parameter.

3 Related Work

This paper contributes to Bayesian deep learning and uncertainty estimation for deep learning.

Bayesian Neural Networks and Uncertainty. Bayesian Neural Networks (BNNs) establish a principled framework for estimating the uncertainty of neural networks by assuming their parameters are latent variables that follow a prior distribution. Bayes’ rule, combined with a likelihood function and observations, defines the posterior distribution of the parameters. However, as exact posterior inference in BNNs is intractable, the problem boils down to approximating the parameter posterior distribution. For example, Markov Chain Monte Carlo (MCMC) [Welling and Teh, 2011, Chen et al., 2014] simulates samples from the posterior distribution, using Langevin [Welling and Teh, 2011] or Hamiltonian [Chen et al., 2014] dynamics. On the other hand, the Laplace approximation [Ritter et al., 2018] applies a second-order approximation at a mode of the posterior distribution.

Variational inference (VI) is a popular approach that reformulates inference as an optimization problem. It seeks the best approximating distribution within a distribution family that minimizes a discrepancy metric to the true posterior, such as the Kullback-Leibler (KL) divergence. Graves [2011] adopt fully-factorized Gaussian posteriors for the network’s parameters, and Blundell et al. [2015] further incorporate the reparametrization trick [Kingma and Welling, 2014, Rezende et al., 2014] to obtain unbiased, low-variance gradient estimates with automatic differentiation. Louizos and Welling [2016] enhance the expressiveness of the posteriors by utilizing matrix Gaussian distributions for structured modeling of parameter correlations within each layer. More recently, Ritter et al. [2021] propose sparse representations of matrix Gaussian posteriors using the idea of inducing points [Snelson and Ghahramani, 2005, Titsias, 2009].

As mentioned above, VI often fails to provide reliable uncertainty estimates in practice [Foong et al., 2019b, Ober and Rasmussen, 2019]. This failure perhaps stems from the disconnect between Bayesian parameter uncertainty and predictive uncertainty—while Bayesian methods focus on

posterior parameter uncertainty, our practical interest lies in estimating the model’s predictive uncertainty. And the gap may be further exacerbated by the variational inference approximation, which involves restrictive independence assumptions [Trippe and Turner, 2017, Foong et al., 2019a, 2020] and mode-seeking behavior of the evidence lower-bound (ELBO) [Bishop, 2006]. Sun et al. [2019] tries to bridge this gap by performing variational inference in the function space, albeit this requires additional approximations to the intractable functional KL divergence. In contrast, the density uncertainty criterion proposed here directly imposes a constraint on the model’s predictive uncertainty, so that the uncertainty is grounded in the empirical density of the input.

Uncertainty Estimation for Deep Learning. This paper proposes a new methodology for estimating uncertainty in deep learning models. Other alternatives for uncertainty estimation include Monte Carlo dropout [Gal and Ghahramani, 2016], which interprets dropout regularization as approximate Bayesian inference and estimates predictive uncertainty by performing Monte Carlo integration using dropout at test time. Variational Gaussian dropout Kingma et al. [2015], motivated by a continuous approximation to dropout [Wang and Manning, 2013], applies multiplicative noise to the preactivations. The authors show this corresponds to assuming a degenerate parameter posterior distribution and provides a variational inference method for adapting the dropout rates. Recently, Dusenberry et al. [2020] propose to model only the uncertainty of rank-1 factors in the network’s parameters and applies multiplicative noise to both the input and the output at each layer.

The neural linear model (NLM) [Snoek et al., 2015, Ober and Rasmussen, 2019, Brosse et al., 2020, Kristiadi et al., 2020] adopts a two-stage approach for deep uncertainty estimation: first, a deterministic neural network is fitted using MAP and then its last layer is replaced with a Bayesian linear layer to estimate the uncertainty. But while NLMs can provide efficient uncertainty estimates [Snoek et al., 2015, Riquelme et al., 2018, Ober and Rasmussen, 2019, Zhou and Precioso, 2019], it’s unclear whether the MAP estimate of the network would necessarily provide meaningful bases for linear uncertainty estimation methods. For example, Thakur et al. [2020], Watson et al. [2021] demonstrate that NLMs fail to capture in-between uncertainties and propose diversity-encouraging regularizers for the representations of the neural network. Liu et al. [2020] try to mitigate the problem by enforcing distance awareness into the network.

While NLMs provide interesting alternatives for uncertainty estimation, we focus on the variational inference methods and related methods [Blundell et al., 2015, Kingma et al., 2015, Gal and Ghahramani, 2016, Dusenberry et al., 2020] that model the uncertainty of the neural network as a whole.

4 Empirical Studies

In this section, we empirically demonstrate that the density uncertainty layer delivers reliable predictive uncertainty estimates. The empirical studies are structured as follows:

1. Visualize the predictive uncertainty landscape of different uncertainty estimation methods on a toy regression problem.
2. Evaluate the uncertainty estimation performance on CIFAR-10/100 classification benchmarks [Krizhevsky and Hinton, 2009] using the ResNet-14 architecture.
3. Evaluate the out-of-distribution (OOD) detection performance on the SVHN dataset [Netzer et al., 2011] using the models trained on CIFAR-10/100 datasets.

Our baselines include the following popular uncertainty methods based on variational inference:

1. **Mean-field Variational Inference** (MFVI) [Blundell et al., 2015] that assume fully factorized normal posteriors on the neural network parameters.
2. **Monte Carlo Dropout** (MCDropout) [Gal and Ghahramani, 2016] that uses dropout as an approximate Bayesian inference method during both training and test times.
3. **Variational Dropout** (VDrop) [Kingma et al., 2015] that applies multiplicative noise to the outputs of linear layers: $a_\ell^j = \epsilon_\ell^j w_\ell^j \cdot h_{\ell-1}$ with $\epsilon_\ell^j \sim \mathcal{N}(1, \alpha)$.
4. **Rank-1 BNN** [Dusenberry et al., 2020] that further extends Variational Dropout by introducing multiplicative noise for both the layer’s input and output, dimension-wise.

Experimental details for CIFAR-10/100 We adopt the standard convolutional ResNet-14 architecture [He et al., 2016] for all methods. We use the ADAM optimizer with learning rate 0.1 except for

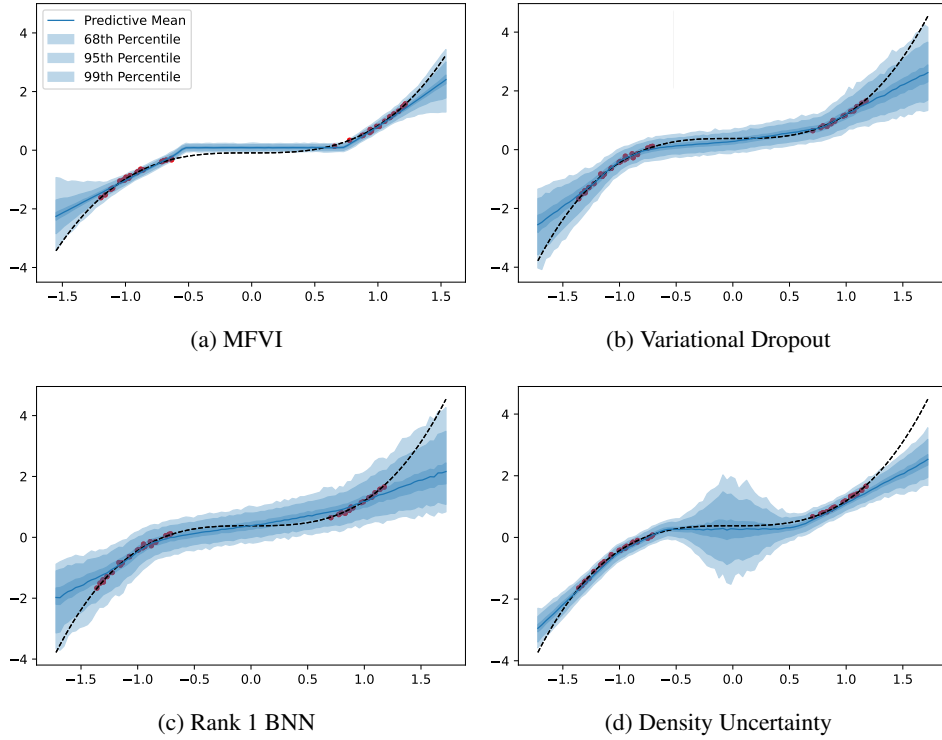


Figure 1: Visualization of predictive uncertainty on a toy regression problem. The red dots denote the training data and the blue shades mark the 68th, 95th, and 99th percentiles of the predictive variance. All baselines other than Density Uncertainty produce unreliable uncertainty estimates, failing to capture the density of the training data

MFVI where the learning rate is reduced to 0.01 as higher learning rate led to divergence. We train the models for 200 epochs with cosine learning rate schedule without restarts [Loshchilov and Hutter, 2017]. During training, we apply random cropping and padding, and horizontal flipping data augmentations. The input pixel values are normalized using the training pixel means and standard deviations, channel-wise. We do not employ KL annealing or posterior tempering but initialize the posterior standard deviation to a sufficiently small value (e.g. 10^{-3}) to stabilize training [Dusenberry et al., 2020]. The weight decay is set to 0.0001 for CIFAR-10 and 0.0002 for CIFAR-100 experiments.

Model-specific hyperparameters are searched on a grid on a randomly sampled held-out set of CIFAR-10. The dropout rate for Monte Carlo Dropout is searched over $\{0.1, 0.2, 0.3\}$ and set to 0.1. For Variational Dropout, we find that adapting the noise variance leads to under-fitting and thus fix the noise variance. The multiplicative noise variance is searched over $\{0.1, 0.25, 0.5\}$ and set to 0.1. For Rank-1 BNN, we assume Gaussian multiplicative noise. The prior standard deviation for the multiplicative noise distributions is searched over $\{0.01, 0.1, 1\}$ and set to 0.1. For Density Uncertainty, the prior noise standard deviation is searched over $\{0.1, 1, 10\}$ and set to 1.

All experiments are implemented in PyTorch [Paszke et al., 2019] and executed on a single Titan X GPU. We submit the source code for the experiments in the supplementary files.

4.1 Toy Regression

We generate a toy regression problem in 1-D to illustrate the predictive uncertainty landscapes of the uncertainty estimation methods. We uniformly sample x_i from $[-4, -2] \cup [2, 4]$ and generate the target as $y_i = x_i^3 + \epsilon$. This leaves a in-between low density region in $[-2, 2]$. We normalize the input and the target to have zero-mean and unit variance. We use MLPs with one hidden layer of width 50.

The predictive uncertainty landscapes are visualized in Figure 1. The visualization shows that the variational inference baselines fail to produce reliable in-between uncertainty in the low density

Table 1: CIFAR-10 classification using 25 posterior samples. The average and the standard deviation over 3 random seeds are shown. Density Uncertainty significantly reduces the calibration error

Method	Accuracy (\uparrow)	ECE (\downarrow)	NLL (\downarrow)
MFVI	91.9 ± 0.1	0.080 ± 0.002	0.291 ± 0.004
MCDropout	91.0 ± 0.1	0.016 ± 0.001	0.261 ± 0.001
VDropout	92.2 ± 0.0	0.013 ± 0.001	0.233 ± 0.002
Rank-1 BNN	92.2 ± 0.0	0.017 ± 0.002	0.231 ± 0.002
Density Uncertainty	92.2 ± 0.3	0.004 ± 0.000	0.226 ± 0.003

Table 2: CIFAR-100 classification using 25 posterior samples. The average and the standard deviation over 3 random seeds are shown. Density Uncertainty significantly reduces the calibration error while improving the other metrics at the same time

Method	Accuracy (\uparrow)	ECE (\downarrow)	NLL (\downarrow)
MFVI	67.9 ± 0.4	0.132 ± 0.002	1.212 ± 0.017
MCDropout	66.3 ± 0.3	0.066 ± 0.001	1.205 ± 0.005
VDropout	67.8 ± 0.1	0.051 ± 0.002	1.167 ± 0.002
Rank-1 BNN	68.0 ± 0.5	0.041 ± 0.003	1.132 ± 0.002
Density Uncertainty	68.8 ± 0.2	0.011 ± 0.003	1.110 ± 0.006

region around the origin. For example, MFVI gives completely collapsed in-between uncertainty while Variational Dropout and Rank 1 BNNs produce flat uncertainty in the in-between low density region. These two methods both apply input-independent noise to the layers and lack a robust mechanism for adjusting their uncertainty depending on the empirical density of the input. On the other hand, Density Uncertainty is able to capture the density of the training data and produce reliable predictive uncertainty. This is because it derives its uncertainty from the density estimate of the input, adhering to the density uncertainty criterion. Notably, it successfully reflects the bimodal nature of the input density even when the individual layer are associated with unimodal Gaussian energy models. This illustrates how the complexity of the uncertainty landscape in density uncertainty layers naturally grows with the number of layers in the neural network.

4.2 Uncertainty Estimation on CIFAR-10 and CIFAR-100

For CIFAR-10/100 experiments, we report test accuracy (Acc), Expected Calibration Error (ECE) [Naeini et al., 2015] and Negative Log-Likelihood (NLL). Expected Calibration Error assesses the quality of the uncertainty estimates by measuring how well-calibrated the model’s predictions are. Negative Log-Likelihood is a proper scoring rule [Gneiting and Raftery, 2007] which favors more accurate and better-calibrated predictions.

The results on CIFAR-10 are summarized in Table 1. Density Uncertainty significantly reduces ECE compared to the baselines while maintaining comparable accuracy and slightly improving NLL. This indicates that Density Uncertainty provides more precise uncertainty estimates with lower calibration error. Table 2 presents the results on CIFAR-100, showing that Density Uncertainty improves the performance on metrics. Notably, Density Uncertainty again reduces ECE significantly. These results validate that Density Uncertainty delivers the most reliable uncertainty estimates among the baselines.

4.3 Out-of-Distribution Detection on SVHN

Table 3 summarizes the the out-of-distribution (OOD) detection performance on SVHN, using the models trained on CIFAR-10/100. We report the area under the precision-recall curve (AUPRC) and the receiver operator characteristic (AUROC). Following the previous work [Ritter et al., 2021], the baselines use the maximum predicted probability for OOD detection. On the other hand, Density Uncertainty, equipped with layer-wise generative energy models, can inherently perform OOD detection using the energy statistics. Specifically, the energy at layer ℓ can be represented as the

Table 3: Out-of-distribution detection performance on SVHN using models trained on CIFAR-10/100. The average and the standard deviation over 3 random seeds are shown. Using the energy statistics, Density Uncertainty shows the most robust out-of-distribution detection performance

Method	CIFAR-10 \rightarrow SVHN		CIFAR-100 \rightarrow SVHN	
	AUPRC (\uparrow)	AUROC (\uparrow)	AUPRC (\uparrow)	AUROC (\uparrow)
MFVI	0.903 ± 0.009	0.830 ± 0.014	0.803 ± 0.008	0.640 ± 0.017
MCDropout	0.892 ± 0.006	0.832 ± 0.010	0.817 ± 0.005	0.666 ± 0.009
VDropout	0.917 ± 0.011	0.866 ± 0.018	0.822 ± 0.028	0.677 ± 0.052
Rank-1 BNN	0.925 ± 0.003	0.880 ± 0.001	0.822 ± 0.027	0.681 ± 0.047
Density Uncertainty	0.952 ± 0.026	0.893 ± 0.056	0.908 ± 0.015	0.800 ± 0.024

squared sum of random variables, based on Equation (21):

$$E_\ell(h_{\ell-1}) = \sum_{j=1}^D (z_\ell^j)^2 \text{ where } z_\ell = \Sigma_{\ell-1}^{-\frac{1}{2}} h_{\ell-1}, \quad (24)$$

where z_ℓ can be thought of as *whitened* input with $\Sigma_{\ell-1}^{-1/2}$ decorrelating the layer’s input $h_{\ell-1}$. By the central limit theorem, this energy tends to be normal-distributed. Therefore, we use the squared deviation of energy from the in-distribution average

$$\|E_\ell(h_{\ell-1}) - \mu_\ell\|_2^2 \quad (25)$$

as a test statistic for OOD detection where the in-distribution average energy μ_ℓ is estimated using a held-out set. We use the energy of the last convolutional layer as it reflects the most high-level, semantic information of the input. Table 3 demonstrates that Density Uncertainty can most robustly detect out-of-distribution input among the baselines.

5 Conclusion

In this paper, we proposed a novel density criterion for reliable uncertainty estimation, asserting that the predictive uncertainty of a model should be grounded in the empirical density of the input. A model that adheres to the criterion will produce higher uncertainty for inputs that are improbable in the training data, and lower uncertainty for those inputs that are more probable. We formalized the concept as a constraint on the predictive variance of a stochastic function and developed the density uncertainty layer as a flexible building block for uncertainty-aware deep learning. Through the empirical studies, we demonstrated that the proposed method provides the most reliable uncertainty estimates and robust out-of-distribution detection performance among the baselines. This could have practical applications in various fields where robust uncertainty estimation is crucial, such as medical diagnosis, autonomous driving, and financial forecasting.

Looking ahead, there are several promising directions for future research. First, exploring the use of mixture noise distributions with heavy tails [Dusenberry et al., 2020] could enhance the model’s robustness against data corruptions and distribution shift [Hendrycks and Dietterich, 2019]. Second, incorporating factorized or low-rank approximations to the energy model may improve the efficiency of the density uncertainty layer. Finally, incorporating Density Uncertainty layer into other deep neural network architectures such as Transformer [Vaswani et al., 2017] could prove effective for building uncertainty-aware models for sequence data such as natural language and times series.

References

- C. M. Bishop. *Pattern recognition and machine learning*. Springer-Verlag New York, Inc., Secaucus, NJ, 2006.
- Charles Blundell, Julien Cornebise, Koray Kavukcuoglu, and Daan Wierstra. Weight uncertainty in neural network. In *ICML*, 2015.

- Nicolas Brosse, Carlos Riquelme, Alice Martin, Sylvain Gelly, and Éric Moulines. On last-layer algorithms for classification: Decoupling representation from uncertainty estimation. *arXiv preprint arXiv:2001.08049*, 2020.
- Tianqi Chen, Emily Fox, and Carlos Guestrin. Stochastic gradient hamiltonian monte carlo. In *ICML*, 2014.
- Dheeru Dua and Casey Graff. UCI machine learning repository, 2017. URL <http://archive.ics.uci.edu/ml>.
- Michael Dusenberry, Ghassen Jerfel, Yeming Wen, Yian Ma, Jasper Snoek, Katherine Heller, Balaji Lakshminarayanan, and Dustin Tran. Efficient and scalable bayesian neural nets with rank-1 factors. In *ICML*, 2020.
- Andrew Foong, David Burt, Yingzhen Li, and Richard Turner. On the expressiveness of approximate inference in bayesian neural networks. In *NeurIPS*, 2020.
- Andrew YK Foong, David R Burt, Yingzhen Li, and Richard E Turner. Pathologies of factorised gaussian and mc dropout posteriors in bayesian neural networks. In *NeurIPS 4th Workshop on Bayesian Deep Learning*, 2019a.
- Andrew YK Foong, Yingzhen Li, José Miguel Hernández-Lobato, and Richard E Turner. ‘in-between’ uncertainty in bayesian neural networks. In *ICML Uncertainty and Robustness in Deep Learning Workshop*, 2019b.
- Yarin Gal and Zoubin Ghahramani. Dropout as a bayesian approximation: Representing model uncertainty in deep learning. In *ICML*, 2016.
- Tilmann Gneiting and Adrian E Raftery. Strictly proper scoring rules, prediction, and estimation. *Journal of the American statistical Association*, 102(477):359–378, 2007.
- Alex Graves. Practical variational inference for neural networks. In *NeurIPS*, 2011.
- Chuan Guo, Geoff Pleiss, Yu Sun, and Kilian Q Weinberger. On calibration of modern neural networks. In *ICML*, 2017.
- Kaiming He, Xiangyu Zhang, Shaoqing Ren, and Jian Sun. Deep residual learning for image recognition. In *CVPR*, 2016.
- Dan Hendrycks and Thomas Dietterich. Benchmarking neural network robustness to common corruptions and perturbations. In *ICLR*, 2019.
- D. P. Kingma and M. Welling. Auto-encoding variational bayes. In *ICLR*, 2014.
- Durk P Kingma, Tim Salimans, and Max Welling. Variational dropout and the local reparameterization trick. In *NeurIPS*, 2015.
- Agustinus Kristiadi, Matthias Hein, and Philipp Hennig. Being bayesian, even just a bit, fixes overconfidence in relu networks. In *ICML*, 2020.
- A. Krizhevsky and G. Hinton. Learning multiple layers of features from tiny images. Technical report, Computer Science Department, University of Toronto, 2009.
- Jeremiah Liu, Zi Lin, Shreyas Padhy, Dustin Tran, Tania Bedrax Weiss, and Balaji Lakshminarayanan. Simple and principled uncertainty estimation with deterministic deep learning via distance awareness. In *NeurIPS*, 2020.
- Ilya Loshchilov and Frank Hutter. Sgdr: Stochastic gradient descent with warm restarts. In *ICLR*, 2017.
- Christos Louizos and Max Welling. Structured and efficient variational deep learning with matrix gaussian posteriors. In *ICML*, 2016.
- Mahdi Pakdaman Naeini, Gregory Cooper, and Milos Hauskrecht. Obtaining well calibrated probabilities using bayesian binning. In *AAAI*, 2015.

- Radford M Neal. *Bayesian learning for neural networks*, volume 118. Springer Science & Business Media, 2012.
- Yuval Netzer, Tao Wang, Adam Coates, Alessandro Bissacco, Bo Wu, and Andrew Y Ng. Reading digits in natural images with unsupervised feature learning. In *NeurIPS Workshop on Deep Learning and Unsupervised Feature Learning*, 2011.
- Sebastian W Ober and Carl Edward Rasmussen. Benchmarking the neural linear model for regression. In *AABI*, 2019.
- Yaniv Ovadia, Emily Fertig, Jie Ren, Zachary Nado, David Sculley, Sebastian Nowozin, Joshua Dillon, Balaji Lakshminarayanan, and Jasper Snoek. Can you trust your model’s uncertainty? evaluating predictive uncertainty under dataset shift. In *NeurIPS*, 2019.
- Adam Paszke, Sam Gross, Francisco Massa, Adam Lerer, James Bradbury, Gregory Chanan, Trevor Killeen, Zeming Lin, Natalia Gimelshein, Luca Antiga, et al. Pytorch: An imperative style, high-performance deep learning library. In *NeurIPS*, 2019.
- Mohsen Pourahmadi. Joint mean-covariance models with applications to longitudinal data: Unconstrained parameterisation. *Biometrika*, 86(3):677–690, 1999.
- D. J. Rezende, S. Mohamed, and D. Wierstra. Stochastic backpropagation and approximate inference in deep generative models. In *ICML*, 2014.
- Carlos Riquelme, George Tucker, and Jasper Snoek. Deep bayesian bandits showdown: An empirical comparison of bayesian deep networks for thompson sampling. In *ICLR*, 2018.
- Hippolyt Ritter, Aleksandar Botev, and David Barber. A scalable laplace approximation for neural networks. In *ICLR*, 2018.
- Hippolyt Ritter, Martin Kukla, Cheng Zhang, and Yingzhen Li. Sparse uncertainty representation in deep learning with inducing weights. In *NeurIPS*, 2021.
- Edward Snelson and Zoubin Ghahramani. Sparse gaussian processes using pseudo-inputs. In *NeurIPS*, 2005.
- Jasper Snoek, Oren Rippel, Kevin Swersky, Ryan Kiros, Nadathur Satish, Narayanan Sundaram, Mostofa Patwary, Mr Prabhat, and Ryan Adams. Scalable bayesian optimization using deep neural networks. In *ICML*, 2015.
- Shengyang Sun, Guodong Zhang, Jiaxin Shi, and Roger Grosse. Functional variational bayesian neural networks. In *ICLR*, 2019.
- Sujay Thakur, Cooper Lorus, Yaniv Yacoby, Finale Doshi-Velez, and Weiwei Pan. Learned uncertainty-aware (luna) bases for bayesian regression using multi-headed auxiliary networks. In *ICML Workshop on Uncertainty in Deep Learning*, 2020.
- Michalis Titsias. Variational learning of inducing variables in sparse gaussian processes. In *AISTATS*, 2009.
- Brian Trippe and Richard Turner. Overpruning in variational bayesian neural networks. In *NeurIPS Approximate Bayesian Inference Workshop*, 2017.
- Aaron Van den Oord, Nal Kalchbrenner, Lasse Espeholt, Oriol Vinyals, Alex Graves, et al. Conditional image generation with pixelcnn decoders. In *NeurIPS*, 2016.
- Ashish Vaswani, Noam Shazeer, Niki Parmar, Jakob Uszkoreit, Llion Jones, Aidan N Gomez, Łukasz Kaiser, and Illia Polosukhin. Attention is all you need. In *NeurIPS*, 2017.
- Sida Wang and Christopher Manning. Fast dropout training. In *ICML*, 2013.
- Joe Watson, Jihao Andreas Lin, Pascal Klink, Joni Pajarinen, and Jan Peters. Latent derivative bayesian last layer networks. In *AISTATS*, 2021.

Max Welling and Yee W Teh. Bayesian learning via stochastic gradient langevin dynamics. In *ICML*, 2011.

Weilin Zhou and Frederic Precioso. Adaptive bayesian linear regression for automated machine learning. *arXiv preprint arXiv:1904.00577*, 2019.

A Additional Experiment Results on UCI Regression

We perform additional experiments on the UCI regression benchmarks [Dua and Graff, 2017], one of the standard uncertainty estimation benchmarks for Bayesian neural networks. We follow the experiment protocol of Gal and Ghahramani [2016]. The benchmark includes regression datasets of varying size (from 300 to 515K) and input dimensions (from 4 to 90), as summarized in Table 6.

Experiment details We follow the experiment protocol of Gal and Ghahramani [2016]. We report the negative log-likelihood (NLL) and the root mean squared error (RMSE) on the test split using 10 posterior samples. For each dataset, the results are averaged over 20 random train-test splits of the data (except for Protein which uses 5 splits and Year which uses a single split). We normalize the input using the mean and the standard deviation of the training split. We use MLPs with two hidden layers of width 50. We increase the width to 100 for the larger datasets of Protein and Year. All models are trained for 100 epochs with learning rate of 0.01 using momentum optimizer. We use batch size of 128 and weight decay of 0.0001. We treat the output variance as a trainable parameter. In order to minimize hyperparameter tuning, we use the same hyperparameters used in the CIFAR-10/100 experiments except that we initialize the posterior standard deviations to a higher value of 0.1 as lower values led to overfitting.

Results Table 4 and Table 5 present the test NLL and the test RMSE on the datasets. Overall, Density Uncertainty gives the best results, outperforming the baselines on 6 of 9 datasets in both NLL and RMSE. These results demonstrate that density uncertainty layers can also bring benefits for regression problems potentially in low-data regimes besides the natural image classification problems studied in the paper. However, a caveat is that the variance of results are still high on some datasets due to their small sizes and the performance on these datasets can be sensitive to the hyperparameters.

Table 4: Test NLL on UCI Regression. Lower is better. The average and the standard deviation over the 20 random train-test splits are shown

Dataset	MCDropout	VDropout	Rank1-BNN	Density Uncertainty
Boston Housing	2.794 \pm 0.141	2.815 \pm 0.092	2.588 \pm 0.236	2.523 \pm 0.205
Concrete Strength	3.533 \pm 0.037	3.497 \pm 0.050	3.112 \pm 0.081	3.093 \pm 0.116
Energy Efficiency	2.604 \pm 0.065	2.525 \pm 0.057	2.044 \pm 0.099	2.034 \pm 0.087
Kin8nm	-0.590 \pm 0.012	-0.792 \pm 0.015	-1.194 \pm 0.028	-1.234 \pm 0.036
Naval Propulsion	-3.437 \pm 0.048	-4.019 \pm 0.008	-4.956 \pm 0.033	-5.274 \pm 0.036
Protein Structure	2.935 \pm 0.006	2.852 \pm 0.005	2.771 \pm 0.010	2.821 \pm 0.001
Wine Quality Red	0.952 \pm 0.062	0.950 \pm 0.067	0.954 \pm 0.108	0.981 \pm 0.109
Yacht Hydrodynamics	3.205 \pm 0.062	3.206 \pm 0.071	2.712 \pm 0.084	2.593 \pm 0.067
Year Prediction MSD	3.568 \pm NA	3.558 \pm NA	3.566 \pm NA	3.570 \pm NA

B Bayesian Neural Networks and Variational Inference

Consider a neural network $\Phi(x; \theta)$ with parameters $\theta = \{w_\ell^j : 1 \leq \ell \leq L + 1, 1 \leq j \leq D\}$ where $\ell = 1, \dots, L + 1$ indexes the layers and $j = 1, \dots, D$ indexes the hidden units in each layer:

$$h_0 = x, \quad (26)$$

$$a_\ell^j = w_\ell^j \cdot h_{\ell-1}, \quad (27)$$

$$h_\ell^j = f(a_\ell^j), \quad (28)$$

$$a_{L+1} = w_{L+1} \cdot h_\ell \quad (29)$$

Here a_ℓ^j is preactivation, h_ℓ^j is activation, \cdot is the dot product, and f is a nonlinear activation function such as ReLU. Bias terms are omitted for simplicity. The likelihood function is parameterized by the neural network output: $p(\mathbf{y}|\Phi(\mathbf{X}; \theta)) = \prod_{i=1}^N p(y_i|\Phi(x_i; \theta))$.

Table 5: Test RMSE on UCI Regression. Lower is better. The average and the standard deviation over the 20 random train-test splits are shown

Dataset	MCDropout	VDropout	Rank1-BNN	Density Uncertainty
Boston Housing	3.715 \pm 0.952	3.710 \pm 0.729	3.212 \pm 0.758	2.957 \pm 0.606
Concrete Strength	7.589 \pm 0.630	7.154 \pm 0.672	5.348 \pm 0.552	5.290 \pm 0.639
Energy Efficiency	3.073 \pm 0.360	3.209 \pm 0.429	1.718 \pm 0.246	1.690 \pm 0.268
Kin8nm	0.121 \pm 0.003	0.094 \pm 0.003	0.073 \pm 0.003	0.070 \pm 0.002
Naval Propulsion	0.007 \pm 0.000	0.003 \pm 0.000	0.010 \pm 0.000	0.001 \pm 0.000
Protein Structure	4.549 \pm 0.033	4.123 \pm 0.028	3.894 \pm 0.046	4.077 \pm 0.043
Wine Quality Red	0.626 \pm 0.046	0.626 \pm 0.049	0.623 \pm 0.051	0.630 \pm 0.050
Yacht Hydrodynamics	5.060 \pm 1.328	4.820 \pm 1.175	3.070 \pm 0.082	2.505 \pm 0.060
Year Prediction MSD	8.726 \pm NA	8.700 \pm NA	8.712 \pm NA	8.710 \pm NA

Table 6: The size and the dimensionality of the UCI regression datasets

Dataset	Size	Dimension
Boston Housing	506	13
Concrete Strength	1,030	8
Energy Efficiency	768	8
Kin8nm	8,192	8
Naval Propulsion	11,934	16
Protein Structure	45,730	9
Wine Quality Red	1,599	11
Yacht Hydrodynamics	308	6
Year Prediction MSD	515,345	90

A Bayesian Neural Network (BNN) assumes a prior over its parameters. A standard choice is an isotropic Normal prior:

$$p(\boldsymbol{\theta}) = \prod_{l=1}^{L+1} \prod_{j=1}^D \mathcal{N}(w_\ell^j | 0, \alpha^{-1} I) \quad (30)$$

The posterior of the parameters given the observations $\mathcal{D} = \{\mathbf{X}, \mathbf{y}\}$ is obtained by the Bayes' rule:

$$p(\boldsymbol{\theta} | \mathcal{D}) \propto \frac{p(\boldsymbol{\theta}) \prod_{i=1}^N p(y_i | \Phi(x_i; \boldsymbol{\theta}))}{p(\mathcal{D})} \quad (31)$$

However, the posterior distribution of parameters $p(\boldsymbol{\theta} | \mathcal{D})$ is highly complex and intractable in BNNs. A popular approach is to approximate the posterior using a parameterized distribution family. For example, a mean-field family assumes fully-factorized Normal distributions:

$$q(\boldsymbol{\theta}) = \prod_{l=1}^{L+1} \prod_{j=1}^D q(w_\ell^j) = \prod_{l=1}^{L+1} \prod_{j=1}^D \mathcal{N}(w_\ell^j | \mu_\ell^j, \text{diag}(\sigma_\ell^j)^2), \quad (32)$$

where $\mu_\ell^j, \sigma_\ell^j$ are the variational parameters. Let $\phi = \{(\mu_\ell^j, \sigma_\ell^j) : 1 \leq l \leq L+1, 1 \leq j \leq D\}$ be the collection of all variational parameters. Variational inference (VI) optimizes the variational parameters to maximize the evidence-lowerbound (ELBO):

$$\mathcal{L}_\phi^{\text{ELBO}} = \mathbb{E}_{q(\boldsymbol{\theta})} [\log p(\mathbf{y} | \Phi(\mathbf{X}; \boldsymbol{\theta})) p(\boldsymbol{\theta}) - \log q(\boldsymbol{\theta})] \quad (33)$$

$$= \mathbb{E}_{q(\boldsymbol{\theta})} [\log p(\mathbf{y} | \Phi(\mathbf{X}; \boldsymbol{\theta}))] - D_{KL}(q(\boldsymbol{\theta}) \| p(\boldsymbol{\theta})) \quad (34)$$

We can show that maximizing the ELBO finds the approximate posterior that minimizes the reverse KL divergence to the true posterior:

$$\mathcal{L}_\phi^{\text{ELBO}} = \mathbb{E}_{q(\boldsymbol{\theta})} [\log p(\mathbf{y} | \mathbf{X}) p(\boldsymbol{\theta} | \mathbf{X}, \mathbf{y}) - \log q(\boldsymbol{\theta})] \quad (35)$$

$$= \mathbb{E}_{q(\boldsymbol{\theta})} \left[\log p(\mathbf{y} | \mathbf{X}) - \log \frac{q(\boldsymbol{\theta})}{p(\boldsymbol{\theta} | \mathcal{D})} \right] \quad (36)$$

$$= \log p(\mathbf{y} | \mathbf{X}) - D_{KL}(q(\boldsymbol{\theta}) \| p(\boldsymbol{\theta} | \mathcal{D})) \quad (37)$$

Once the variational parameters are fitted, the BNN’s predictive posterior for test input x_* can be estimated with Monte Carlo samples from the approximate posterior $q(\theta)$:

$$p(y_*|x_*, \mathcal{D}) = \int p(y_*|x_*, \theta)p(\theta|\mathcal{D})d\theta \approx \int p(y_*|x_*, \theta)q(\theta)d\theta = \mathbb{E}_{q(\theta)}[p(y_*|x_*, \theta)]. \quad (38)$$

In practice, however, VI frequently fails to generate reliable uncertainty estimates for BNNs, as we illustrated using a simple toy problem in the paper. The fundamental cause may stem from the discrepancy between estimating the uncertainty of parameters and the model’s predictive uncertainty. While VI approximates the uncertainty of the parameters, it remains unclear how this approximation influences predictive uncertainty. This issue is further compounded by the restrictive independence assumptions and mode-seeking behavior of the ELBO. To provide reliable uncertainty estimates for deep learning, we proposed to directly regulate the predictive uncertainty based on the estimated density of the inputs.

C Bayesian Uncertainty in Linear Classification

In the paper, we demonstrated that the Bayesian uncertainty for linear regression is grounded in the density estimate of input. But how about in classification? We show that the Bayesian uncertainty in classification is also based on a density estimate but with a weighted generative objective.

We consider a logistic classification problem, with the input $\mathbf{X} \in \mathbb{R}^{N \times D}$, the target $\mathbf{y} \in \mathbb{R}^N$, and the weight $w \in \mathbb{R}^D$:

$$p(w) = \mathcal{N}(w|0, \alpha^{-1}I), \quad (39)$$

$$p(\mathbf{y}|\mathbf{X}, w) = \prod_{i=1}^N y_i^{\sigma(w \cdot x_i)} (1 - y_i)^{1 - \sigma(w \cdot x_i)}, \quad (40)$$

where σ is the logistic sigmoid function: $\sigma(x) = 1/(1 + e^{-x})$. Although the exact posterior distribution is intractable in this case, we can obtain a Gaussian approximation using the Laplace’s approximation [Bishop, 2006]:

$$q(w) = \mathcal{N}(w|\mu_{\text{MAP}}, \Lambda^{-1}), \quad (41)$$

$$\Lambda = \sum_{i=1}^N \sigma(w \cdot x_i)(1 - \sigma(w \cdot x_i))x_i x_i^T + \alpha I, \quad (42)$$

and μ_{MAP} is the MAP estimate of the weight. Comparing the posterior precision (Equation (42)) to that of the regression in the paper $\Lambda = \beta \sum_i x_i x_i^T + \alpha I$, we find that the precision matrix in classification is a *weighted* estimate of the input covariance. Noting that the weight $\sigma(w \cdot x_i)(1 - \sigma(w \cdot x_i))$ is higher for inputs with more uncertain predictions (i.e., $\sigma(w \cdot x_i)$ is closer to 0.5), Bayesian classification prioritizes inputs that give higher prediction uncertainty, in contrast to the regression case where all inputs were weighted uniformly. Recall that the posterior precision essentially serves as a Gaussian density estimate of the input. Equation (42) shows that Bayesian logistic classification performs weighted generative modeling of the input, and by prioritizing inputs that are more informative, it can potentially better utilize the capacity of the Gaussian energy model.

Despite this finding, in the paper we chose to use the unweighted generative objective for density uncertainty layers because (1) the weighted objective can lead to an unfaithful estimate of the input density and (2) the capacity of the generative model was not a major concern in our case, as the complexity of the uncertainty landscape naturally grows with the number of layers in the network.

References

- C. M. Bishop. *Pattern recognition and machine learning*. Springer-Verlag New York, Inc., Secaucus, NJ, 2006.
- Charles Blundell, Julien Cornebise, Koray Kavukcuoglu, and Daan Wierstra. Weight uncertainty in neural network. In *ICML*, 2015.

- Nicolas Brosse, Carlos Riquelme, Alice Martin, Sylvain Gelly, and Éric Moulines. On last-layer algorithms for classification: Decoupling representation from uncertainty estimation. *arXiv preprint arXiv:2001.08049*, 2020.
- Tianqi Chen, Emily Fox, and Carlos Guestrin. Stochastic gradient hamiltonian monte carlo. In *ICML*, 2014.
- Dheeru Dua and Casey Graff. UCI machine learning repository, 2017. URL <http://archive.ics.uci.edu/ml>.
- Michael Dusenberry, Ghassen Jerfel, Yeming Wen, Yian Ma, Jasper Snoek, Katherine Heller, Balaji Lakshminarayanan, and Dustin Tran. Efficient and scalable bayesian neural nets with rank-1 factors. In *ICML*, 2020.
- Andrew Foong, David Burt, Yingzhen Li, and Richard Turner. On the expressiveness of approximate inference in bayesian neural networks. In *NeurIPS*, 2020.
- Andrew YK Foong, David R Burt, Yingzhen Li, and Richard E Turner. Pathologies of factorised gaussian and mc dropout posteriors in bayesian neural networks. In *NeurIPS 4th Workshop on Bayesian Deep Learning*, 2019a.
- Andrew YK Foong, Yingzhen Li, José Miguel Hernández-Lobato, and Richard E Turner. ‘in-between’ uncertainty in bayesian neural networks. In *ICML Uncertainty and Robustness in Deep Learning Workshop*, 2019b.
- Yarin Gal and Zoubin Ghahramani. Dropout as a bayesian approximation: Representing model uncertainty in deep learning. In *ICML*, 2016.
- Tilman Gneiting and Adrian E Raftery. Strictly proper scoring rules, prediction, and estimation. *Journal of the American statistical Association*, 102(477):359–378, 2007.
- Alex Graves. Practical variational inference for neural networks. In *NeurIPS*, 2011.
- Chuan Guo, Geoff Pleiss, Yu Sun, and Kilian Q Weinberger. On calibration of modern neural networks. In *ICML*, 2017.
- Kaiming He, Xiangyu Zhang, Shaoqing Ren, and Jian Sun. Deep residual learning for image recognition. In *CVPR*, 2016.
- Dan Hendrycks and Thomas Dietterich. Benchmarking neural network robustness to common corruptions and perturbations. In *ICLR*, 2019.
- D. P. Kingma and M. Welling. Auto-encoding variational bayes. In *ICLR*, 2014.
- Durk P Kingma, Tim Salimans, and Max Welling. Variational dropout and the local reparameterization trick. In *NeurIPS*, 2015.
- Agustín Kristiadi, Matthias Hein, and Philipp Hennig. Being bayesian, even just a bit, fixes overconfidence in relu networks. In *ICML*, 2020.
- A. Krizhevsky and G. Hinton. Learning multiple layers of features from tiny images. Technical report, Computer Science Department, University of Toronto, 2009.
- Jeremiah Liu, Zi Lin, Shreyas Padhy, Dustin Tran, Tania Bedrax Weiss, and Balaji Lakshminarayanan. Simple and principled uncertainty estimation with deterministic deep learning via distance awareness. In *NeurIPS*, 2020.
- Ilya Loshchilov and Frank Hutter. Sgdr: Stochastic gradient descent with warm restarts. In *ICLR*, 2017.
- Christos Louizos and Max Welling. Structured and efficient variational deep learning with matrix gaussian posteriors. In *ICML*, 2016.
- Mahdi Pakdaman Naeini, Gregory Cooper, and Milos Hauskrecht. Obtaining well calibrated probabilities using bayesian binning. In *AAAI*, 2015.

- Radford M Neal. *Bayesian learning for neural networks*, volume 118. Springer Science & Business Media, 2012.
- Yuval Netzer, Tao Wang, Adam Coates, Alessandro Bissacco, Bo Wu, and Andrew Y Ng. Reading digits in natural images with unsupervised feature learning. In *NeurIPS Workshop on Deep Learning and Unsupervised Feature Learning*, 2011.
- Sebastian W Ober and Carl Edward Rasmussen. Benchmarking the neural linear model for regression. In *AABI*, 2019.
- Yaniv Ovadia, Emily Fertig, Jie Ren, Zachary Nado, David Sculley, Sebastian Nowozin, Joshua Dillon, Balaji Lakshminarayanan, and Jasper Snoek. Can you trust your model’s uncertainty? evaluating predictive uncertainty under dataset shift. In *NeurIPS*, 2019.
- Adam Paszke, Sam Gross, Francisco Massa, Adam Lerer, James Bradbury, Gregory Chanan, Trevor Killeen, Zeming Lin, Natalia Gimelshein, Luca Antiga, et al. Pytorch: An imperative style, high-performance deep learning library. In *NeurIPS*, 2019.
- Mohsen Pourahmadi. Joint mean-covariance models with applications to longitudinal data: Unconstrained parameterisation. *Biometrika*, 86(3):677–690, 1999.
- D. J. Rezende, S. Mohamed, and D. Wierstra. Stochastic backpropagation and approximate inference in deep generative models. In *ICML*, 2014.
- Carlos Riquelme, George Tucker, and Jasper Snoek. Deep bayesian bandits showdown: An empirical comparison of bayesian deep networks for thompson sampling. In *ICLR*, 2018.
- Hippolyt Ritter, Aleksandar Botev, and David Barber. A scalable laplace approximation for neural networks. In *ICLR*, 2018.
- Hippolyt Ritter, Martin Kukla, Cheng Zhang, and Yingzhen Li. Sparse uncertainty representation in deep learning with inducing weights. In *NeurIPS*, 2021.
- Edward Snelson and Zoubin Ghahramani. Sparse gaussian processes using pseudo-inputs. In *NeurIPS*, 2005.
- Jasper Snoek, Oren Rippel, Kevin Swersky, Ryan Kiros, Nadathur Satish, Narayanan Sundaram, Mostofa Patwary, Mr Prabhat, and Ryan Adams. Scalable bayesian optimization using deep neural networks. In *ICML*, 2015.
- Shengyang Sun, Guodong Zhang, Jiabin Shi, and Roger Grosse. Functional variational bayesian neural networks. In *ICLR*, 2019.
- Sujay Thakur, Cooper Lorus, Yaniv Yacoby, Finale Doshi-Velez, and Weiwei Pan. Learned uncertainty-aware (luna) bases for bayesian regression using multi-headed auxiliary networks. In *ICML Workshop on Uncertainty in Deep Learning*, 2020.
- Michalis Titsias. Variational learning of inducing variables in sparse gaussian processes. In *AISTATS*, 2009.
- Brian Trippe and Richard Turner. Overpruning in variational bayesian neural networks. In *NeurIPS Approximate Bayesian Inference Workshop*, 2017.
- Aaron Van den Oord, Nal Kalchbrenner, Lasse Espeholt, Oriol Vinyals, Alex Graves, et al. Conditional image generation with pixelcnn decoders. In *NeurIPS*, 2016.
- Ashish Vaswani, Noam Shazeer, Niki Parmar, Jakob Uszkoreit, Llion Jones, Aidan N Gomez, Łukasz Kaiser, and Illia Polosukhin. Attention is all you need. In *NeurIPS*, 2017.
- Sida Wang and Christopher Manning. Fast dropout training. In *ICML*, 2013.
- Joe Watson, Jihao Andreas Lin, Pascal Klink, Joni Pajarinen, and Jan Peters. Latent derivative bayesian last layer networks. In *AISTATS*, 2021.

Max Welling and Yee W Teh. Bayesian learning via stochastic gradient langevin dynamics. In *ICML*, 2011.

Weilin Zhou and Frederic Precioso. Adaptive bayesian linear regression for automated machine learning. *arXiv preprint arXiv:1904.00577*, 2019.